Modes of Grain Growth in Cold Rolled 3.25% Al-Fe Alloys With and Without Dopant S

Hitoshi NAKAE*
Noriaki GOSHI**

(Received July 27, 1973)

Abstract

In the modes of grain growth in cold rolled 3.25% Al-Fe alloy sheet, some points still remained to be explained. In the first point, the growth curves obtained experimentally are rather complicated in contrast to the simple exponential curve anticipated from a driving force based on the grain boundary energies constituted by an aggregate of small grains formed in primary recrystallization. In the second point, the texture with (100) [001] orientation as the main component is formed in Al-Fe, whereas (110) [001] is seen in Si-Fe during the growth stage from nearly the same textures in as-rolled and primarily recrystallized states of both alloys.

The authors assumed a local deviation in compositions from nominal ones along the grain boundaries possibly motivated by boundary migration, and have associated them with a characteristic point of phase diagrams of the alloy systems at which a local phase transition (e. g. from solid to liquid) in a region of deviated composition along grain boundaries could occur.

Based on the above the behavior of growth may be described by a characteristic rate and habit of growth in tne presence of a liquid phase and thereupon a complicated course in growth curves in the alloys and a preferential growth of (100) [001] component in Al-Fe alloy sheet could reasonably be explained.

I. Introduction

The recrystallization texture of 3.25% Al-Fe alloy sheet is known to consist of a main component of (100) [001] in contrast to that of (110) [001] orientation in 3.25% Si-Fe alloy sheet, while they show similar physical properties with regard to electrical resistivity, magnetic permeability, and mechanical tensile behaviors[1),2)].

In the recrystallization of Si-Fe alloy sheets, the main component of the texture has been known to be strengthened by a small addition of sulfur, titanium, niobium etc[3)~7)]. The effects of sulfur, and manganese have been reported by May, Turnbull and one of the present authors[8)~10)].

* Department of Precision Engineering, Faculty of Engineering, Hokkaido University, Sapporo, Japan.
** Division of Precision Engineering, Graduate School of Engineering; now assigned to Hitachi Kinzoku Co., Kawagoe, Tokyo, Japan.

It is also known, that the texture in Si-Fe alloy under certain conditions has (100) [001] component as the main component, e.g. in grain growth in thin sheet or often at an annealing temperature exceeding 1200°C[11)~13)].

It would be worthwhile to discuss the effect of sulfur on the grain growth behavior in Al-Fe alloy with the special reference to the results obtained in Si-Fe alloy containing sulfur and to elucidate the mechanism involved which leads to cause the difference in growth behaviors in Al-Fe and Si-Fe alloys.

II. Experimental procedure

The specimens were melted in a vacuum furnace by adding different amounts of sulfur to 3.17% Al-Fe base alloy. After hot working, they were cold rolled until the final thickness of 0.35 mm. The reduction estimates 75%. The chemical compositions are listed in Table 1. in which the content of sulfur was 0.004, 0.060, and 0.148% in No. 1, 2, and 3, respectively. No sulfur was doped in the No. 1 specimen and the high content of carbon in No. 3 specimen was due to the carbon contained in the doped sulfur material which might give no essential effect on the results.

The specimens were annealed and observed at 50°C from 600 to 700°C and at 100°C intervals from 700 to 1200°C with an isochronal annealing time of 1 hour. Optical microscope, Gonio-microscope[14)], X-ray and torque magnetometer were employed for the observation of structures and the determination of textures.

TABLE 1 Chemical composition of the Al-Fe alloy specimens (wt %)

	Al	C	Si	S	P	Bal.
No. 1	3.17	0.007	0.01	0.004	0.002	Fe
No. 2	3.17	0.009	0.01	0.060	0.002	Fe
No. 3	3.17	0.030	0.04	0.148	0.002	Fe

III. Experimental results

The textures were determined by X-ray method in the three specimens with various sulfur contents in cold rolling, primary recrystallization and the grain growth, a qualitative analysis of the shift rate of the textures during grain growth was made by observations of magnetic torque curves together with the X-ray pole figures.

1) Textures as rolled

The pole figures are shown in Fig. 1 (A), (B) and (C) in which the textures are constituted by the three major components of (112) [1$\bar{1}$0], (111) [11$\bar{2}$] and (100) [011]. The (110) [001] and (100) [001] components which will become the major components of recrystallization texture thereafter were observed by the orientation etch-pit method using a Gonio-microscope, and it was found that their concentrations became sharper with the increased sulfur doping.

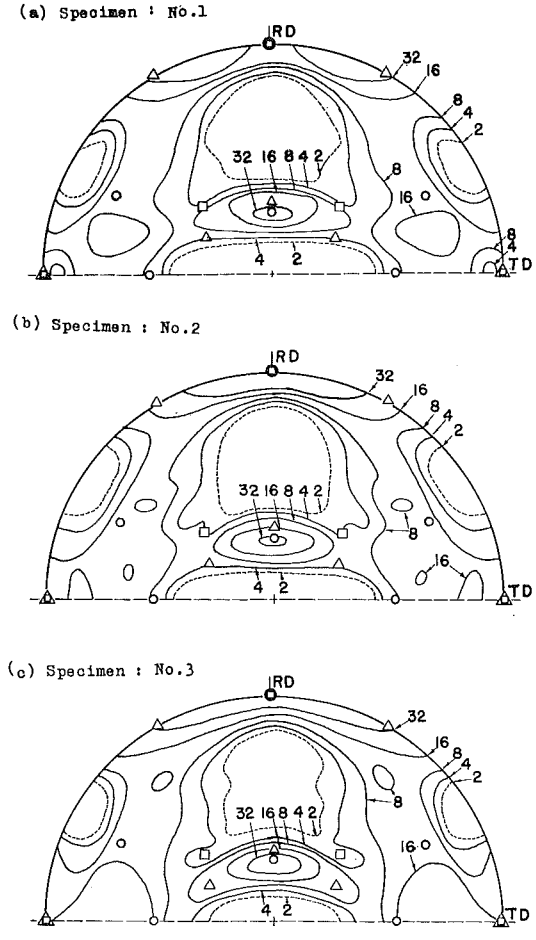

Fig. 1. (110)-pole figures of cold rolled 3.17% Al-Fe alloy sheets by 70% to 3.5 mm in thickness. Symbols △, ○ and □ indicate (111) [11$\bar{2}$], (112) [1$\bar{1}$2] and (100) [011] poles respectively.

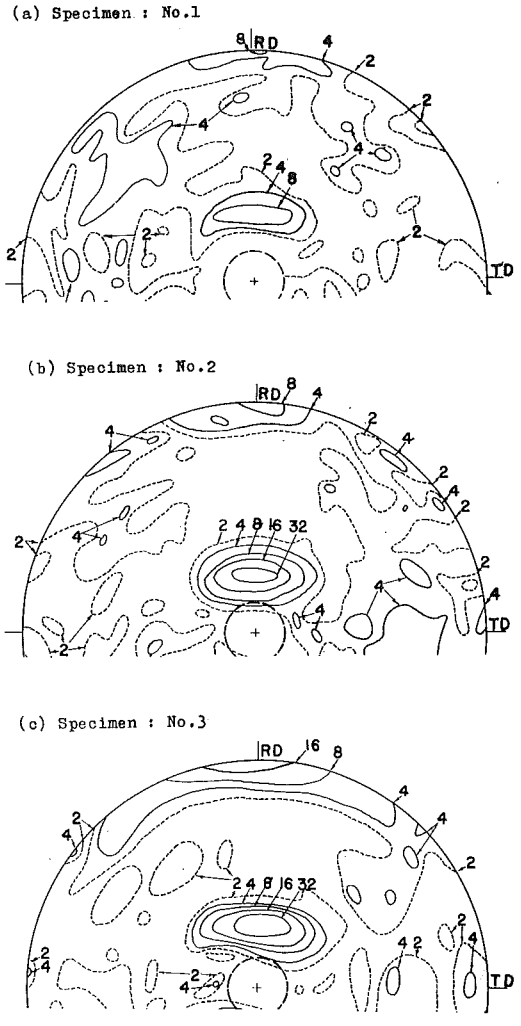

Fig. 2. (110)-pole figures of cold rolled 3.17% Al-Fe alloy sheets annealed at 700°C for 1 hr in hydrogen atomosphere.

2) Primary recrystallization textures

The textures of these three specimens are shown in Fig. 2 (A), (B), and (C), annealed at 700°C for 1 hour which seems to be at a step generally expressed as primary recrystallization. The components constituting the texture are of the same components as cold rolled texture of (112) [1$\bar{1}$0], (111) [11$\bar{2}$], (110) [001], (100) [001], and a fairly large part of random components, with a rather increased spread though the (112) [1$\bar{1}$0], (111) [11$\bar{2}$] and (110) [001] components are strengthened by the addition of sulfur. By optical microscopic observation, a major part of (110) [001] and (100) [001] components are of recrystallized grains, while other

components are still in the recovery stage.

In any event the cold rolled and primarily recrystallized textures of 3.25% Al-Fe alloy may be considered to be essentially similar to those observed in cold rolled 3.25% Si-Fe alloy with the same effect of sulfur.

In a 3.25% Si-Fe alloy sheet, each component of the same orientation appeares as a group forming a colony or flora in each orientation and among them the (110) [001] and (100) [001] components existed near the surface of the sheet with small orientation spread, whereas the (111) [11$\bar{2}$] and (112) [1$\bar{1}$0] components existed in the inner part of the specimen with a rather large orientation spread.

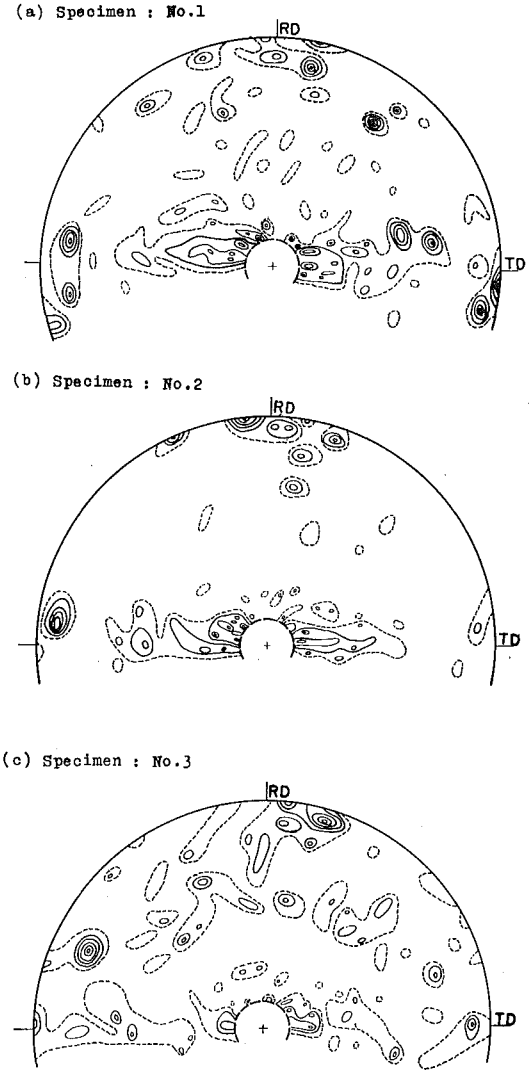

Fig. 3. (100)-pole figures of cold rolled 3.17% Al-Fe alloy sheets annealed at 1200°C for 1 hr in hydrogen atomosphere.

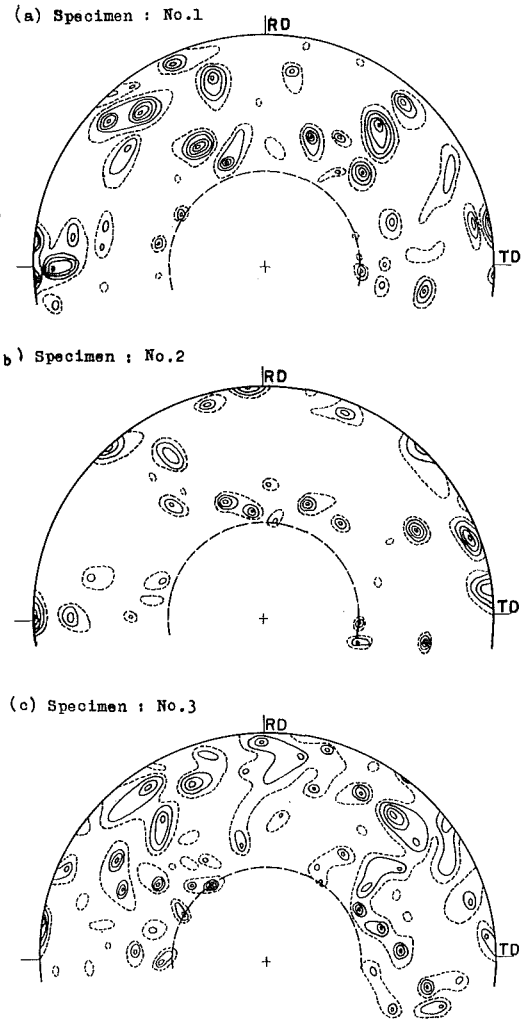

Fig. 4. (110)-pole figures of cold rolled 3.17% Al-Fe alloy sheets annealed at 1200°C for 1 hr in hydrogen atomosphere.

Then the formers are known to grow dominantly against the latters at the stage of grain growth[10]. These behaviors may also be expected to occur in Al-Fe alloy sheet.

3) Textures during and after grain growth

(*i*) *Pole figure*

The pole figures of (100)- and (110)- poles on on the specimens, annealed at 1200°C for 1 hour are shown in Fig. 3 (A), (B) and (C), and Fig. 4 (A), (B) and (C) respectively. In the figures, the growth seems to be carried both in (110) [001] and (100) [001] components by the consumption of other residual components, in contrast to the 3.25% Si-Fe alloy sheet whose growth component is mainly a (110) [001] orientation.

In the No. 1 specimen, the texture is composed of two main components of (110) [001] and (100) [001] with a weak (112) [$1\bar{1}0$], (111) [$11\bar{2}$] and a dispersed (100) [011]. In the No. 2 specimen, the main components are the same as in No. 1, but other components are hardly seen. In the No. 3 specimen, the main components are also the same as in the above two specimens, however (111) [$11\bar{2}$] and (100) [011] components are seen at a very small degree. In these three specimens in common, the (110) [001] and (100) [001] components which form the main part of texture are seen with a slight dispersion of orientation around the common [001] axis.

(*ii*) *Magnetic torque curve*

The magnetic torque curves were taken on the specimens annealed at the temperatures from 650°C up to 1200°C and a tendency of texture shift during grain growth was observed qualitatively. Although a magnetic torque curve of a polycrystalline specimen is the statistical mean of basic curves for the orientations of all the crystals, the effects of several preferred orientations will be considered briefly referring to Fig. 5[13].

For (100) [001] crystal, the magnetic torque L is given by

$$L = -(K_1/2)\sin 4\alpha\,,$$

for (100) [011] crystal which is one of the components of the deformation texture and an orientation obtained by a rotation of 45° from the above crystal,

$$L = (K_1/2)\sin 4\alpha\,,$$

and for (110) [001] crystal,

$$L = -(K_1/4)\sin 2\alpha - (3K_1/8)\sin 4\alpha\,,$$

where K_1 is the first anisotropic constant, α the direction cosine of [001] direction referred to the X axis of the three dimensional coordinate. In this case, other direction cosines of β and γ referred to Y and Z axes disappear. The second anisotropic constant K_2 was neglected because of its meager contribution to the torque value. The torque values of other components such as (111) [$11\bar{2}$] and

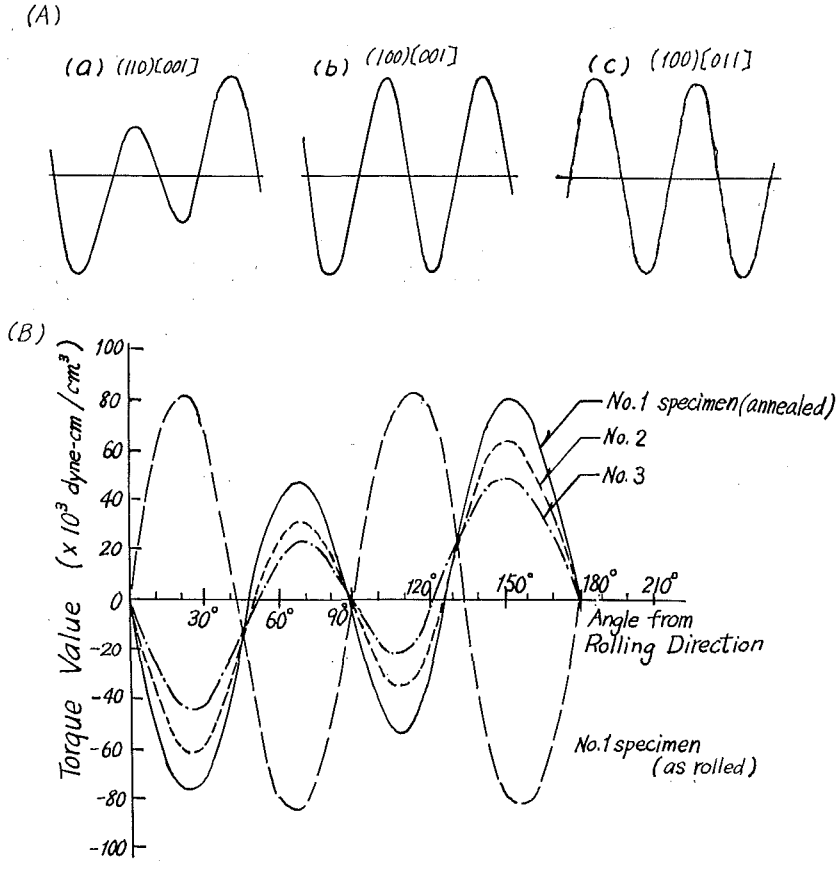

Fig. 5. Torque curves of a few typical single crystals (A) and of cold rolled 3.17% Al-Fe alloy sheets of as rolled and annealed at 700°C for 1 hr in hydrogen atomosphere (B).

(112) [1$\bar{1}$0] orientations will also be neglected in the analysis for the same reason.

As for the (110) [001] and (100) [001] orientations the torque curves are in phase, therefore, maximum torque values are associated to the degree of alignment of the (110) [001] plus (100) [001] components. The (100) [011] component is anti-phase to the former two components, hence its existence in the texture diminishes the maximum torque values markedly. As for the quantitative balance of the (110) [001] and (100) [001] components in the texture, the ratio of the maximum values of the first to the second may be estimated, since they are 0.43 and unity with (110) [001] and (100) [001] orientations respectively. The magnetic torque curves taken for the specimens over the entire range of recrystallization show the characteristic curve shape of (110) [001] plus (100) [001] components and thereon the analysis will be made. In the primary recrystallization, the maximum torque values show a decrease with the increased sulfur doping, while the torque ratios are large and almost the same in No. 1 and 2 and small in No. 3 as seen in Fig. 6 (A) and (B). They will be explained together with the pole figures in

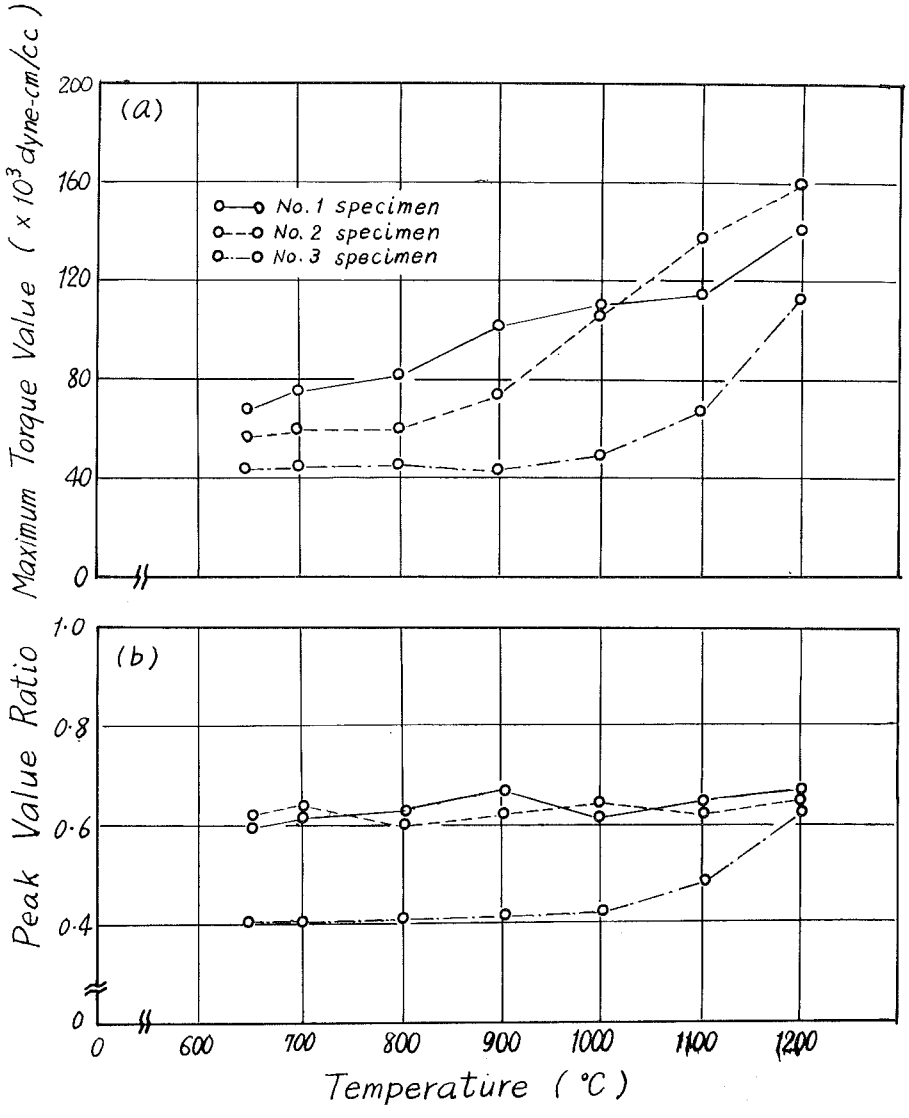

Fig. 6. Maximum torque values (a) and peak value ratios (b) of cold rolled 3.17% Al-Fe alloy sheets annealed at various temperatures for 1 hr in hydrogen atomosphere.

Fig. 3 as having (110) [001], (100) [001] and (111) [11$\bar{2}$] and (100) [011] components which exist commonly in these three specimens and the former two components occupy a large part of the specimens in which the (110) [001] is the most dominant.

As for the tendencies of quantitative balance of (110) [001] and (100) [001] components in the textures during the growth, a torque ratio versus temperature curves in Fig. 6 (B) may be considered. A increase of the torque ratio against temperature would mean that the growth of the (100) [001] component was

dominant over the (110) [001] component during growth. The tendency was most marked in the No. 3 specimen. Here the growth of these major components may be achieved by absorbing the other components such as (111) [11$\bar{2}$], (1$\bar{1}$2) [1$\bar{1}$0], (100) [011] and others existing in the primary recrystallization texture. These tendencies may be characteristic only in Al-Fe alloy and somewhat different from those in Si-Fe alloy whose dominant growth component has a (110) [001] orientation[10].

The maximum torque values at raising temperatures show at first a direct increase in the No. 1 specimen presenting no sulfur practically, while remaining unvaried uptill 800°C and 1000°C in the No. 2 of moderate sulfur and the No. 3 of the highest sulfur respectively. Then, a retardation of growth beginning at 900°C is observed in No. 1, whereas no retardation is seen in No. 2 containing sulfur. (also in No. 3 specimen)

The (111) [11$\bar{2}$] and (112) [1$\bar{1}$0] components consisting a main part of as rolled texture remain slightly in No. 1 and considerably higher in No. 3, while they are hardly seen in No. 2 specimen annealed at 1200°C for 1 hour.

IV. Discussion

The grain growth involving a grain boundary migration in alloys is compared to the crystallization or crystal growth of many other substances (e.g. ionic or homo-polar) in which crystals grow from a vapor or liquid as well as from a solid phase[16]. In these substances, a growing crystal generally tends to be free of defects and foreign atoms, and crystallization is known to be one of the ways

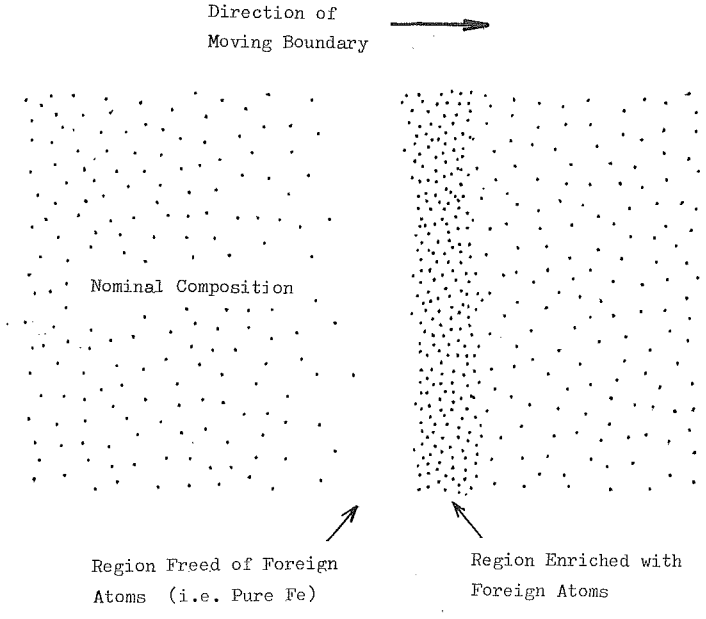

Fig. 7. Regions of deviated compositions from nominal one afterward and forward of moving boundary (Schematic)

of purifying materials. The tendency may be due to the familiarity of interactions between respective like atoms and foreign atoms which are transported to meet by grain boundary migration. It may not be unreasonable to extend the thinking also to a grain growth in alloys. Then, the hinter and forward regions of a moving boundary could tend to be of free and rich regions of foreign atoms respectively (cf. Fig. 7).

In the case of Al-Fe and Al-S-Fe alloy systems, a foreign atom may imply the alloying addition Al as well as the doped element sulfur. In the course of achievement of grain growth, the inner part of the moving boundary will become rather pure Fe, while the outer region may be enriched by Al and S.

This phenomenon may be a tendency against a thermodynamical or phase equilibrium. Then, for the sake of high atomic diffusivity in metals, the regions with deviated compositions from nominal one will become a transient and minute layer inside and outside the moving boundaries. If either one of these regions meet the characteristic points or transition lines corresponding to its deviated composition on the phase diagrams of the alloys at raising temperatures, they will be subjected to a phase transformation in the alloys in which no transformation appears until an intersection with a solidus line over 1500°C in nominal compositions. Then, the alloy can meet the A_3 point, eutectic points and solidus line in their deviated compositions at the stage of grain growth. If a liquid phase appears in a grain boundary, the grain growth will be obeyed by a general feature of crystal growth in the presence of a liquid phase[17)~19)] for which much work on the characteristic rate and habit of growth has been reported.

For the discrimination of the process, the phase diagrams of ternary Al-S-Fe alloy system should be referred to. But we have, however, no sufficient information concerning this, it is referred to the diagrams of each binary alloy system of Al-Fe and S-Fe, assuming that the characterstic points of these binary alloy diagrams will be linked with the characteristic points of the ternary systems to some extent and also give some significant knowledges on the effects[7)].

Now, the growth curves expressed by a torque maximum and a torque ratio will be referred to the phase diagrams of the binary alloy systems[20)] (cf. Fig. 8). The retardation of growth observed on the torque maximum begins at 900°C in plain Al-Fe alloy which has also been observed in Si-Fe alloy coincides with A_3 transformation in pure Fe at 910°C. It may be deduced that at the inner region of moving boundaries, the alloy may tend to be rather pure iron and may give rise to A_3 transformation or stagnation of boundary migration. The fact that no retardation is observed in Al-Fe alloy doped sulfur will support the above explanation, since only a small addition of S to Fe degenerates the A_3 transformation drastically as seen in the phase diagram of S-Fe system.

The increased rate of growth and the growth of (100) [001] component observed at 1000°C in Al-Fe alloy doped sulfur which is also observed as a growth of single (110) [001] component in Si-Fe alloy[15)] may be associated to the eutectic point of 988°C in Fe-FeS system. The coincidence of another eutectic point at

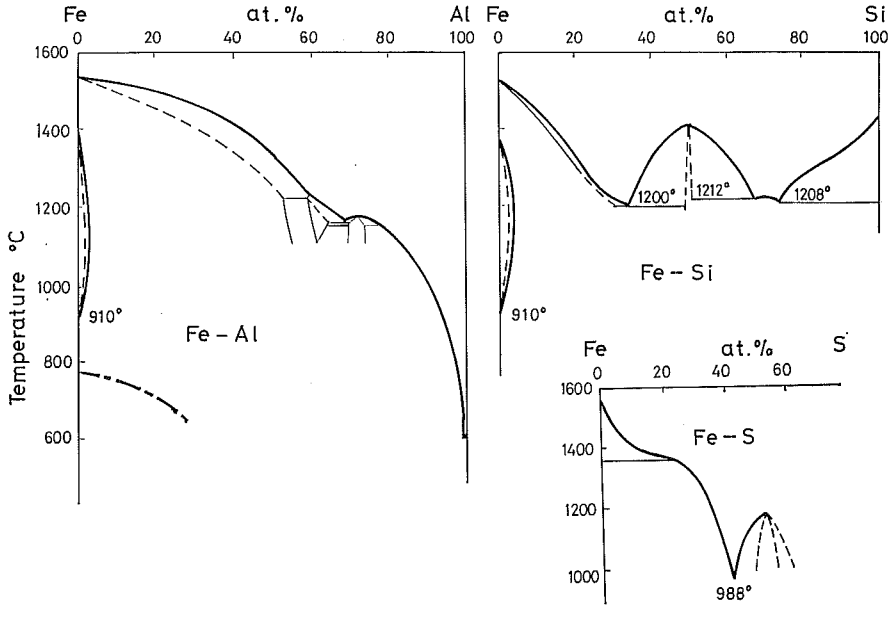

Fig. 8. Phase diagrams of alloy system of Fe-Al, Fe-Si and Fe-S[20].

1160°C to the growth would appear, if the plots against temperature were taken precisely around the point, though it was not obvious on the curves.

A mode of crystal growth in the presence of a liquid phase may be compared to the dendritic growth in a cast ingot of iron whose direction and plane of growth relative to a crystal coincide with ⟨100⟩ direction and {100} plane respectively.

In the grain growth in alloys, the process may, however, be carried in a two-fold manner, firstly to minimize an interfacial energy which depends chiefly on the geometry of interfaces and then to satisfy the preference for growth in crystallographic planes between the grains facing each other.

As for the growth of (100) [001] component in Al-Fe alloy in the growth stage, it may be ascribed to the lower solidus line against temperature in the Al rich side of the phase diagram to the extremity of 660°C of melting point of Al. The effect will, however, be integrated and become conspicuous although occurring in a minute region, because the reacting regions travel through the matrix following the migrating boundaries.

Another remark will be made here to the effect that the temperature at which the growth of (100) [001] component begins in Si-Fe alloy also corresponds to the eutectic points 1200, 1208 and 1212°C of the alloy.

V. Conclusion

The conclusions brought about from the experimental results on the texture formation in cold rolled 3.17% Al-Fe alloy with or without doped sulfur will be

summarised as follows.

(1) The as-rolled and primarily recrystallized textures were essentially the same at each stage as those observed in 3.25% Si-Fe alloy regardless of sulfur content, being

(i) the as-rolled textures were composed of (112) [$1\bar{1}0$], (111) [$11\bar{2}$], (100) [001] and other random components in the descending order of concentration and

(ii) the primarily recrystallized textures were composed of nearly the same components of as-rolled textures with a rather increased spread, appearing a (110) [001] component as minute but distinctly recrystallized one.

(2) During the grain growth, the (110) [001] plus (100) [001] components grew commonly in the alloys with or without doped sulfur in which the growth of (100) [001] components was dominant over that of (110) [001] in contrast to Si-Fe alloy whose dominant component during growth was of a single (110) [001] orientation.

(3) In view of the association of the growth behaviors in alloys to the crystal growth or crystallization in other substances, the origination of liquid phase along moving boundaries and thereupon the mode of grain growth in the presence of a liquid phase were proposed.

The modes of grain growth in Al-Fe alloy sheet may eventually be attributed to the presence of a liquid phase in the stage of, or in the temperature range of grain growth and the effect of sulfur as the dopant should also be discussed in the same situation. However, the prominent contribution by Taguchi and Sakakura will also be one of the influential proofs for the growth of cube texture in Al-Fe alloy[21].

For the confirmation of above conclusions especially on (3) term, the experiments on other alloys entailing the similar energy process as well as the precise plots of growth curves in Al-Fe alloys were undertaken with affirmative results.

Acknowledgement

The authors acknowledge their indebtedness to Profs. K. Nishida, K. Matsubara and T. Matsushita for the helpful advices and discussions.

References

1) R. M. Bozorth, Ferromagnetism Van Nostrand Comp., Inc., New York **58** (1953), 219.
2) I. Gokyu, H. Abe, T. Hashida and S. Takahashi: J. Japan Inst. Metals, **25** (1961), 712.
3) H. Fiedler: Trans. Met. Soc. AIME, **221** (1961), 1201.
4) H. Fiedler: ibid., **227** (1963), 776.
5) H. Fiedler: J. Appl. Phys., **29** (1958), 361.
6) E. W. Walter and J. Howard: J. Iron and Steel Inst., **194** (1960), 96.
7) N. G. Ainslie and U. Seybolt: ibid., **194** (1960), 341.
8) J. May and D. Turnbull: Trans. AIME, **212** (1958), 769.

9) J. May and D. Turnbull: J. Appl. Phys., **30** (1959), 210.
10) H. Nakae and K. Tagashira: Trans. Japan Inst. Metals, **14** (1973), 15.
11) F. Assmuss, K. Detert and G. Ibe: Z. Metallk., **48** (1957), 344.
12) G. W. Wiener: J. Appl. Phys., **35** (1964), 856.
13) G. Wiener, P. A. Albert, R. H. Trapp and M. F. Littmann: ibid., **29** (1958), 366.
14) T. Taoka, E. Furubayashi, and S. Takeuchi: Japanese J. Appl. Phys., **4** (1965), 120.
15) F. Brailsford: Magnetic Materials, Methuen Publs. Co., London (1960), 65.
16) See for example: Ed. by A. Van Hook: Crystallization, Reinhold Publ. Corp., Chapman and by and Hall Ltd., London, (1961).
L. S. Peiser: Crystal Growth, Pergamon Press, New York, (1966).
17) W. D. Kingery: J. Appl. Phys., **30** (1959), 301.
18) W. D. Kingery, M. D. Narasimhan: ibid., **30** (1959), 307.
19) W. D. Kingery, E. Niki, M. D. Narasimhan: J. Amer. Ceram. Soc., **44** (1961), 29.
20) M. Hansen, K. Anderko: Constitution of Binary Alloys, McGraw-Hill Book Co., New York, (1958).
21) S. Taguchi and A. Sakakura: Acta Met., **14** (1966), 405.